The Role of Irrigation in Determining the Global Land Use Impacts of Biofuels*

by

Farzad Taheripour**
Thomas W. Hertel
Jing Liu

GTAP Working Paper No. 65
2011

* Acknowledgement: We are deeply indebted to Ximing Cai for his contributions to this work. We had valuable discussions and meetings with him that significantly improved quality of this work. We would like to thank Stefan Siebert for providing data on global cropland and crop production by irrigation type which made this research possible. This research is partially funded by the USDA and DOE grants.

**Corresponding author: 403 W. State St., West Lafayette, IN 47907, phone: 765-494-4612, email: tfarzad@purdue.edu. Farzad Taheripour is energy economist, Thomas W. Hertel is distinguished professor, and Jing Liu is Ph.D. student in the Department of Agricultural Economics at Purdue University.

THE ROLE OF IRRIGATION IN DETERMINING THE GLOBAL LAND USE IMPACTS OF BIOFUELS

Abstract

In recent years there has been a flurry of activity aimed at evaluating the land use consequences of biofuels programs and the associated carbon releases. In this paper we argue that these studies have tended to underestimate the ensuing land use emissions, because they have ignored the role of irrigation, and associated constraints on cropland expansion. In this paper, we develop a new general equilibrium model which distinguishes irrigated and rainfed cropping industries at a global scale. Using the new model we evaluate the implications of land use change due to US ethanol programs, in the context of physical constraints on the expansion of irrigated cropland. We find that models which mingle irrigated and rainfed areas underestimate the global land use changes induced due to the US ethanol expansion by about 5.7%. They tend to underestimate the corresponding land use emissions by more than one fifth.

The Role of Irrigation in Determining the Global Land Use Impacts of Biofuels

1. Introduction

Previous research into the global land use impacts of biofuels has assumed that cropland area could expand in most regions of the world. Such estimated expansion into more carbon-rich land cover such as grassland or forest is the focus of recent research into the contributions of indirect land use changes (ILUC) to the GHG impacts of biofuels. Several studies have examined the global land use consequences of biofuel production (e.g. Gurgel et al., 2007; Searchinger, et al., 2008; Hertel et al., 2010, Taheripour et al., 2010, Tyner et al. 2010, and Taheripour et al., 2011). However, all of these studies have effectively treated all cropland as being rainfed. The role of irrigation in biofuel-induced cropland expansion has been wholly ignored. This could introduce systematic biases in the measurement of indirect land use emissions due to production of biofuels.

Irrigated croplands typically have much higher yields than their rainfed counterparts in the same country/Agro Ecological Zone (AEZ). Thus, the question of whether expansion of global cropland cover involves irrigated or rainfed lands makes a significant difference in terms of how much new land will be required to provide the additional production called for in the presence of biofuels. If the new lands are irrigated, and therefore have higher yields than rainfed lands in the same AEZ, then less land conversion will be required. However, if expansion of irrigated area is constrained, either due to insufficient water, or due to insufficient capacity, then the answer could be quite different. In general, since irrigated yields exceed rainfed yields, if expansion of irrigation is constrained, it is likely that more cropland area will be required to meet the additional global demand induced by ethanol production.

A recent report by McKinsey & Co (2009), offers an assessment of water availability over the coming two decades, drawing heavily on the IFPRI water model (Cai and Rosegrant, 2002). They start at the river basin level and calculate water demand based on current technology and expected growth in agricultural and industrial output as well as population. In the absence of efficiency gains, they estimate that water demand will exceed existing sustainable, reliable water supply by 40% in 2030. Furthermore, this global gap masks much more serious water gaps at the level of individual river basins. They estimate that one-third of the world's population in 2030 will live in basins where the projected gap is greater than 50 percent. In summary, it appears that water for agricultural irrigation will become much more expensive in the future – no doubt spurring considerable efficiency gains, but also raising the cost of production and sharply limiting the amount of land on which crops can be economically grown.

In addition to leading to an understatement of global area requirements, omitting explicit analysis of irrigation, and associated constraints, is likely to shift the distribution of land use changes towards dry (currently irrigated) regions with lower land use emission factors (less above-ground carbon). In the presence of irrigation constraints the distribution of land use changes induced by biofuel production will shift towards areas where expansion of rainfed agriculture is possible. These regions tend to be more carbon rich and therefore exhibit higher emissions factors. Hence, earlier models which ignore the role of irrigation in crop expansion tend to underestimate the ILUC emissions due to biofuel production. In this paper we explore the impacts of water constraints on the ILUC emission estimates due to US ethanol production.

To accomplish this task, given the fact that a large-scale expansion in biofuels affects a broad range of economic activities at a global scale, a global Computational General Equilibrium (CGE) model is developed building on the recent work of Taheripour, Hertel, and Tyner (2011:

henceforth THT). Those authors developed a global CGE model which handles production, consumption and trade of biofuels along with other economic activities, and which is capable of tracing the land use impacts of expansion in biofuels. Similar to most other models used for this purpose, THT ignores the role of irrigation. In this paper, we remedy this previous limitation.

We begin by modifying the GTAP Data Base to distinguish irrigated and rainfed agriculture. Here we follow the pioneering work of Portmann et al. (2010: henceforth PDS) who develop a land use data base which provides data on harvested area and crop production by 29 crops and 160 countries/regions at the 0.5x0.5 degree grid cell level. These spatially disaggregated data are aggregated to the level of 18 GTAP-AEZs, while maintaining the distinction between irrigated and rainfed crops. Using the information obtained from this data set, all crop industries presented in the v.6 GTAP Data Base are broken into irrigated and rainfed categories.

In the second step, the GTAP-BIO-AEZ model used in THT is extended and modified to handle production, consumption, and trade of irrigated and rainfed crops. To accomplish this task, all components of the GTAP-BIO-AEZ model including: production, demand, and supply functions as well as market clearing conditions are revisited. In this revised model, it is assumed that, for each crop, the irrigated and rainfed industries produce the same commodity (e.g. wheat) which enters the market and sells for the same price. This homogeneity assumption means that it is possible for irrigated production of any given crop to be completely eliminated if competition for irrigated land is sufficiently intense in a given region. This is an important distinction from the modeling approach of Alvarado et al. (2011) which assumes that irrigation water is simply one of many inputs into a national production function.

This revised model is used to conduct a series of experiments which permit us to revisit the global land use impacts of biofuels expansion, comparing the findings to those previously obtained while ignoring the distinction between irrigated and rainfed agriculture. The first experiment assumes that there is no water constraint across the world and that irrigated area can be expanded wherever economic incentives dictate, in response to expanded US ethanol production. In the second experiment, we impose a set of water scarcity constraints, defined based on information from the International Water Management Institute (IWMI). These prevent expansion of irrigated area in regions where physical water scarcity is currently active. The ILUC results associated with these two models are found to bracket the results generated when failing to distinguish rainfed and irrigated agriculture.

In what follows, we first review the literature on land use changes due to biofuel production. Then we explain construction of a new GTAP Data Base which we build to accomplish objective of this paper. After that we introduce modifications which were made in the GTAP-BIO-AEZ model to handle production of irrigated and rainfed crops. The next section defines our experiments and introduces areas where irrigation cannot be expanded due to water scarcity. Then we present the simulation results. The last section provides conclusions.

2. Literature Review

Land use changes and their consequent emissions induced by crop expansion due to biofuel production have proven to be a controversial topic, resulting in a rapidly proliferating literature. The early papers suggested that biofuel production could have extraordinary land use implications (Searchinger et al. 2008, Fargione et al. 2008). Figure 1 shows that more recent studies find the early estimates to have overstated the land use implications of US ethanol production (Hertel et al., 2010, Taheripour et al., 2010, and Tyner et al., 2010). Searchinger et

al. (2008) provided the first peer-reviewed estimate for the ILUC (about 0.73 hectares of new cropland area per 1000 gallon of ethanol capacity). Those authors used a partial equilibrium modeling framework (FAPRI) to assess the ILUC due to US ethanol program. After that Hertel et al. (2010) using a general equilibrium model showed that full accounting for market mediated price responses to ethanol production, as well as the geography of world trade, contributed to significant reductions in estimated ILUC impacts. Those authors estimated that the ILUC for the US ethanol program is about 0.29 hectares per 1000 gallons of ethanol. In more recent work THT made several changes in the GTAP-BIO modeling framework and its data base and used the improved model to examine consequences of biofuel mandates for the global livestock industry. These authors projected that the US and EU biofuel mandates will jointly expand the global cropland area by 11.8 million hectares, but they have not evaluated the ILUC due to mandates of each region. In another line of research in this area Tyner et al. (2010) have extended the model developed in THT and provided three sets of estimates for the ILUC due to the US ethanol. As shown in Figure 1, the estimates provided by Tyner et al. (2010) are significantly lower than provided in Hertel et al. (2010). Several modifications, including assigning higher productivity rates to new croplands (obtained from the Terrestrial Ecosystem Model (TEM)), and establishing a new baseline contributed to these further reductions.

The right hand axis and the blue bars in Figure 1 compare estimates of land use emissions due to US ethanol for each of these studies. This figure indicates that the most recent estimates for the land use emissions are also significantly lower than the earlier estimates. The estimates for the land use emissions due to US ethanol have followed a downward path from about 100 grams/MJ (estimated by Searchinger et al., 2008) to 14.5 grams/MJ (estimated by Tyner et al., 2010).

Despite this extensive work to date seeking to better understand the land use implications of biofuels, no attempt has been made to examine the role of irrigation in biofuel-induced cropland expansion[1]. This paper expands the capability of the GTAP modeling framework which have been extensively used in land use assessments of biofuels, to disaggregate irrigation activities.[2]

3. Data Base Construction

In this paper we extend the GTAP-BIO-AEZ data base used in Taheripour et al. (2011) to incorporate crop industries by irrigation type. In so doing, we rely on the pioneering work done by PSD who develop a data base which provides data on harvested area and yield by irrigation type for 29 groups of crops and 160 countries/regions at the 0.5x0.5 degree grid cell level. We achieved this split through two steps which are explained in sequence below.

3.1 Determining harvested area and crop production by irrigation type

Based on the PSD data set we divided the harvested area and crop production of the SAGE/GTAP data base documented in Monfreda et al. (2008), into two categories of rainfed and irrigated (for details see Appendix A). The new data base collapses all types of crops into 8 GTAP commodities and represents the harvested area and crop production by country, AEZ, and irrigation type.

Tables A2 and A3 of Appendix A summarize the new data set at an aggregated (19 region[3]) level. In this table we sum harvested areas and crops outputs over all types of crops and

[1] Some studies including Fraiture et al. (2008), Hoogeveen et al. (2009), and Dominguez-Faus et al. (2009) have examined water implications of producing biofuels at regional and global levels.
[2] In this paper we use the modeling framework developed in THT as our starting point. The model provided by these authors is not the latest version of GTAP-BIO, but it has almost all modifications which are confirmed through a peer-reviewing process.
[3] These 19 regions and their members are defined in appendix B.

all AEZs. In this newly constructed data base, about 23% of the global harvested area is irrigated, while global irrigated lands account for about 38% of global agricultural outputs (measured by weight). This indicates that irrigated lands are more productive versus rainfed lands. The global average yields for irrigated and rainfed areas are about 10.8 mt/ha and 5.3 mt/ha.

To understand the role of irrigation in crop production, we review the new data base from different angles. First, consider the geographical distribution of harvested area and crop production regardless of irrigation type. Table A2 shows that about 57% of global harvested areas belong to India (14.3%), China (12.6%), Sub Saharan Africa (10.7%), US (10.3%), and EU (9%) regions. Table A3 represents global distribution of crop production. This table indicates that the shares of India and Sub Saharan Africa in global crop production are about 9.5% and 4.4%, respectively. These figures are less than the shares of these regions in global harvested area. The share of China in global crop production is about 14.4%, moderately higher than its share in global harvested area. However, the shares of US and EU in global crop production are about 15% and 15.2% which are considerably higher than their shares in global harvested area. This indicates that the US and EU croplands are physically more productive compared to the world average productivity of land.

Now consider the global distributions of harvested area and crop production by irrigation type. Table A2 and Figure 2 indicate that about 60.3% of global rainfed harvested areas belong to Sub Saharan Africa (13.3%), India (11.6%), US (11.3%), EU (10.6%), and China (9%). Table A3 and Figure 3 show the global distribution of the rainfed crop production. They indicate that the shares of Sub Saharan Africa and India in the rainfed crop production are respectively about 5.9% and 5.4%, respectively. These figures are significantly lower than their corresponding

shares in the harvested rainfed areas. However, the shares of US and EU in the global rainfed crop production are about 16.2% and 20.5%, which are significantly larger than their shares in the global rainfed harvested areas. These figures indicate that productivities of the rainfed crops in these two regions (in particular in EU) are relatively higher than the world average.

Consider now the global distributions of harvested area and crop production for irrigated practices. Table A2 and Figure 2 show that more than 65% of the global irrigated areas belong to the Asian countries and regions, including such as China (24.6%), India (23.2%), and all countries located in South East Asia (18%). After these regions, the largest area of irrigated land belongs to the US which owns about 7.2% of the global irrigated areas. On the other hand, Table A3 and Figure 3 indicate that China, India, and US supply about 16%, 16%, and 13% of irrigated crops, respectively. These figures show that, while China and India control about half of the global irrigated areas, they account only for 32% the global irrigated crops.

We now use Figure 4 to analyze the harvested area and crop production within each region by irrigation type. The left panel of this figure indicates the shares of irrigated and rainfed harvested areas in each region. This panel indicates that agricultural activities in some regions like Canada, Russia, and Sub Saharan Africa are mainly relied on rainfed. On the other hand, counties located in Asia are relied more on irrigation.

The right panel on Figure 4 represents shares of irrigated and rainfed crops in each region. The share of irrigated crop is higher than the share of irrigated land in each region and all regions presented in Figure 4, except for Japan and China. This shows that in general irrigated areas are more productive than their counterpart rainfed areas in each region.

To investigate differences in yield between rainfed and irrigated lands consider Figure 5. This figure shows that irrigated croplands typically have much higher yields than their rainfed

counterparts in each region. This figure shows that in Brazil there is a major difference between the yields of irrigated and rainfed lands. This is due to the fact that irrigated sugarcane provides much better yield than the rainfed. In preparing Figure 5 we summed up harvested areas and outputs over all types of crops and AEZ. To examine differences between the irrigated and rainfed yields by crops now consider Figure 6 which shows differences between the irrigated and rainfed yields for six crop categories for the major crop producer countries of US, EU, China, and India. This figure shows that in all of these counties irrigated and rainfed yields are different for each and every crop. It also indicates that yields are usually higher in US for almost all crops, with few exceptions. EU yields for the irrigated oilseeds and the rainfed wheat are higher than other regions. Among these 4 regions, India has the lowest yields for all 6 crop categories.

Figure 6 shows that the US rainfed and irrigated national yields are not very different for coarse grains. However, this is clearly a function of compositional effects, since, as Figure 7 shows, US rainfed and irrigated coarse grains at the AEZ level are very different. The largest differences between the rainfed and irrigated coarse grains yields arise in the drier AEZs, including AEZ7, AEZ8, AEZ13, AEZ14, which produce irrigated corn. However, in the Midwest areas where the rainfed corn is the dominant crop (mainly AEZ10 and AEZ11) there is no major difference between the irrigated and rainfed yields suggesting that irrigation in these regions is largely an occasional supplement to normally ample rainfall.

3.2 Splitting GTAP Data Base

The next step in constructing the irrigation-augmented model is to divide each and every crop activity in the GTAP data base into two crop industries representing irrigated and rainfed production using the *SplitCom* program (Horridge, 2005). We establish the split process based on the following assumptions. First, we assume that the irrigated and rainfed products are

homogeneous. This means that the price of rainfed wheat and irrigated wheat are the same, and so on for other crops. Second, we assume that the rainfed and irrigated crop producers pay the same price for a given input. This means that, for example, the price of seed is the same for both producers. Third, we assume that the input-output ratio is the same for both rainfed and irrigated production. This means that the same amount of fertilizer is required to produce a ton of wheat, regardless of whether it is irrigated or rainfed. When combined with the equal output and input price assumptions, this implies that the cost shares are the same for each input used in the two industries. For example, the cost share of labor in the irrigated wheat industry must be the same as the cost share of labor in the rainfed wheat industry. Since the value of output per hectare will be higher on irrigated land (due to higher yields), and since the share of this higher value going to land is the same as for rainfed land, then the returns to irrigated land will also be higher.

These assumptions provide a theoretical basis for using *SplitCom* to divide each and every crop industry of GTAP into two distinct industries of irrigated and rainfed. The *SplitCom* program needs exogenous information on the shares of irrigated and rainfed industries in the sales, costs, and trade items of each crop industry to carry out the split process in each region (Horridge, 2005). To provide the required exogenous information, we calculated the shares of irrigated and rainfed quantities of production of each crop in total production of that crop. Then we run the *SplitCom* program sequentially to split each and every crop industry of GTAP into two distinct industries of irrigated and rainfed. Note that these procedures are made at the most disaggregated level of GTAP Data Base and then we aggregate the results to the 19 region level used in this paper.

4. Modification of the GTAP-BIO model

The standard GTAP modeling framework uses a one to one relationship between industries and commodities. This means that in the standard framework each industry produces only one commodity and each commodity is produced only by one industry. The GTAP-BIO modeling framework extended this tradition and considers production of two commodities by a single industry in order to handle biofuel by-products (Taheripour et al. 2010). In this paper we extend the GTAP-BIO model so that each crop could be produced by two different industries, one irrigated and one rainfed. In this model it is assumed that for each crop the irrigated and rainfed industries produce the same commodity (e.g. wheat) which enters the market and sells for the same price. This homogeneity assumption means that it is possible for irrigated production of any given crop to be completely eliminated if competition for irrigation is sufficiently intense in a given region. In particular, we introduce the following percentage change form equations into the model to handle production of one homogeneous commodity by two distinct industries:

$$pi_{irrigated_j} = pi_{rainfed_j} = ps_j, \ for\ all\ j \in set\ of\ crop\ commodities, \quad (1)$$

$$pi_j = \sum_{k \in top\_com}^{K} S_{jk} * pf_{jk} \ \ for\ all\ j \in crop\ industries\ set, \quad (2)$$

$$qf_{jk} = qi_j - \varepsilon\left[pf_{jk} - pi_j\right] for\ all\ k \in top\_com\ set\ and\ all\ j \in crop\ industries\ set, \quad (3)$$

$$qo_c = \sum_{w \in irrigated,rainfed} supplyshr_{cw} * qi_w \ \ for\ all\ c \in crop\ commodity\ set. \quad (4)$$

In the above equations *pi* and *qi* represent percent changes in the price and quantity of *j* at the industry level and *ps* and *qo* represent their corresponding percentage changes at the commodity market level (where there is no distinction made about method of production). The variables *qf* and *pf* stand for percentage changes in prices and quantities of inputs used for crop production at the industry level. Finally, S_{jk} represents the cost share of input *k* in industry *j*, ε is

the elasticity of substitution among intermediate inputs, and $supplyshr_{cw}$ is the share of crop c supply by irrigation type *w*.

Equation (1) ensures that irrigated and rainfed industries which produce the same crop (e.g. wheat) will receive the same price and that the prices at the industry and commodity levels are the same. Equation (2) is the zero profit condition for each crop industry. Equation (3) represents the demand for intermediate input k in crop industry j, and finally equation (4) ensures market clearing condition for each crop.

In addition, we redesigned the land supply function used in the GTAP Model. The standard land supply tree in GTAP-AEZ consists of two levels. The lower nest of this three determines distribution of land cover across forest, pastureland, and cropland. The top nest governs supply of cropland to crop activities and determines distribution of this type of land among all crop activities. To handle allocation of cropland among irrigated and rainfed agriculture, a new supply tree is defined (Figure 8). As shown in this figure the lower level operates the same as the standard model. It allocates land cover among forest, pastureland, and cropland categories. The second level of the new structure allocates cropland between irrigated and rainfed cropping activities. Finally, the top level of the new tree governs the supplies of irrigated and rainfed areas among the irrigated and rainfed cropping activities, separately[4].

5. Experimental Design

To analyze the role of irrigation in determining the global land use consequences of biofuels we undertook three experiments. In the first experiment, we use the modeling framework developed in THT to assess the land use impacts of ethanol production. This

[4] In addition to the above changes we made the necessary changes in the GTAP code to support production of crops by irrigation type.

experiment represents earlier work which failed to distinguish between irrigated and rainfed lands. Henceforth, we refer to this case as *mingled experiment*.

The second and third experiments are built based on the new model developed in this paper. In the second experiment, it is assumed that there is no water constraint anywhere in the world; if so desired, irrigated land can be expanded as long as it is profitable. Henceforth, we refer to this case as *unconstrained experiment*.

Finally, in the third simulation we limit expansion of irrigation in those areas where water supply is limited and cannot be expanded. To accomplish this task we rely on the data provided by IWMI[5]. This institute provided a map which shows water scarcity across the world. The map distinguishes three groups of water scarcity. The first two groups represent the areas which are currently facing with physical water scarcity or approaching to this constraint. The third category shows the areas which are facing with economic constraints to use water resources (Map 1). In this paper we collapsed the first two types of water scarcity to determine the regions which are facing with water limits and hence we assume that irrigation cannot be expanded in those areas. Since economic constraints are built in the GTAP Data Base, we *do not* impose any *a priori* restriction on the expansion of irrigation in the areas are indicated as being constrained for economic reasons. Henceforth, we refer to this case as *constrained experiment*.

In all experiments developed in this paper we simulate the land use consequences of an increase in US ethanol production from its 2001 level to 15 billion gallons, which is the mandated level of ethanol for 2015. Following Hertel et al. (2010), in these experiments we only shocked US ethanol to isolate impacts of US ethanol production from other factors which shape the world economy. In these experiments we also use the same elasticities and parameters as

[5] This data is taken from Smakhtin (2011).

used in THT. The only exception is related to the newly introduced land transformation elasticity between the irrigated and rainfed croplands in the land supply tree. To represent a fluid movement between the irrigated and rainfed cropland in response to economic incentives we set Ω_2=10. This high value of the land transformation elasticity facilitates land conversion from rainfed areas to irrigated areas if the latter become relatively more profitable in the wake of increased ethanol production.

Simulation results

5.1 Land use changes

Table 1 compares the regional land use changes obtained from the experiments defined in the previous section. This table indicates that as we move from the *unconstrained* case to the *constrained* case the land use impacts of biofuel increases. An increase in the US ethanol production from its 2001 level to 15 billion gallons requires about 3.75 million hectares additional cropland when there is no water constraint. Under the *constrained* cases the magnitude of the land requirement increases to 4.4 million hectares. The land use requirement for the *mingled* case is about 4.2 million hectares and therefore falls in between the results for the *unconstrained* and *constrained* cases. The magnitudes of the land requirement per 1000 gallons of ethanol for the *unconstrained, mingled,* and *constrained* cases are about 0.28, 0.32, and 0.33. These results confirm that earlier studies which mingled the irrigated and rainfed and ignored the fact that irrigated areas cannot be expanded in many regions across the world underestimate the land use impacts of US ethanol production by about 5.7%. The results obtained from the *unconstrained* and *constrained* cases indicate that the imposition of realistic irrigation constraints increases the size of land requirement by 18% compared.

The results also show that the presence of irrigation constraints alters the geographic pattern of land use change in the wake of the US ethanol expansion. For example, table 1 indicates that the irrigation constraint significantly expands the shares of the US, Canadian, and Sub Saharan African regions, while reducing that for Other-CEE-CIS.

The composition of land conversion also changes when we move from the *unconstrained* case to the *constrained* one. Since rainfed agriculture is more likely than irrigated agriculture to compete with forest, the *constrained* case shows greater conversion of forest compared to the *unconstrained* case globally (up from 28.9% in the *unconstrained* case to 31.5% in the *constrained* case, see Table 2). However, the share of forest in the US does not vary significantly across these two cases. Table 2 indicates that the mingle case significantly underestimates the share of forest in the US cropland expansion.

We now examine the distribution of changes in cropland by rainfed vs. irrigated agriculture. Table 3 shows that in the *unconstrained* case ethanol production increases mainly global irrigated areas by about 3.7 million hectares (about 98.6% of total). In this experiment regions such as US, EU27, China, and members of Other_CEE_CIS expands their irrigation areas while reduce their rainfed activities. On the other hand in this experiment some regions such as Brazil, Canada, and Sub Saharan Africa increase their irrigated and rainfed areas together.

The irrigation constraint reduces the global irrigated areas from 3.7 million hectares to 1.3 million hectares and increases the global rainfed areas from a negligible magnitude to 3.2 million hectares. In the *constrained* case the EU27 expands its irrigated areas by 1.1 million hectares. In this case most of the regions mainly expand their rainfed areas.

While tables 1 to 3 show the overall land use impacts of ethanol production under alternative assumptions about the potential for irrigation expansion, the picture at the AEZ level is more complex. To examine the impacts of the irrigation constraint on the geographic pattern of land use within US, consider Table 4 which reports differences between the changes in the cropland areas of this region by AEZ obtained from the *unconstrained* and *constrained* cases. This table indicates that, when there is no irrigation constraint, the irrigated areas in AEZ7 and AEZ8 go up significantly in response to higher demand for corn. About 50% of US irrigated area resides in these two AEZs where the yield difference between irrigated and rainfed cropping activities is very high. Hence, when there is no irrigation constraint, ethanol production converts rainfed areas to irrigated areas in these two AEZs. On the other hand as shown in table 4, ethanol production changes irrigated areas barely in AEZ9, AEZ10, and AEZ11. These AEZs mainly represent the Midwest of US where rainfed cropping activities are very fertile and irrigation contributes only modestly to yield increases. In general, expansion in corn demand increases corn supply at the costs of reduction in the productions of other crops. In this process when there is no irrigation constraint, the irrigated corn industry expands its production in the areas where irrigation significantly contributes to production (i.e. AEZs 7 and 8). On the other hand the rainfed corn industry mainly expands its activities in Midwest where irrigation is not an issue.

When irrigation is constrained, the irrigated corn industry cannot expand its activities in the AEZs where irrigation is critical to production. On the other hand, in the rainfed AEZs, the profitability of irrigated agriculture does not rise as sharply as for rainfed production and therefore, irrigated area does not experience the same strong expansion. Instead, as shown in table 4, it is the rainfed corn industry that expands strongly in this area.

Maps 2 also report the change in cropland cover across the world owing to increased ethanol production in the US for the *unconstrained* and *constrained cases*. In these maps figures represent changes in harvested irrigated and rainfed areas at the Region/AEZ level. These maps illustrate that the irrigation constraint significantly alters the geographical distribution of irrigated and rainfed areas across the world.

5.2 Land use emissions

To calculate land use emissions due to the US ethanol production for the cases developed in this paper we rely on the land use emissions factors provided by Plevin et al. (2011). These authors developed a model, augmented with a series of land use emissions factors, which gauge carbon fluxes due to land use changes induced by biofuel production at the AEZ level at a global scale. Map 3 demonstrates the land use emission factors for forest and pasture lands. These maps show that the land use emissions factors vary across the world and land type, significantly. For example the top panel of this map shows that the Malaysian and Indonesian forest areas have very large carbon fluxes compared to other regions across the world. The maps also indicate that the carbon fluxes are very different across AEZs within each region as well. For example, the forest emissions factor of the US AEZ 7 (which covers a large area in the west side of US) is about 469 Mg CO2 ha^{-1}. The corresponding forest emissions factors for the US AEZ9, AEZ10 and AEZ11 (which covers Midwest) are higher than this figure by 30.4%, 40.2% and 58.2%. These figures show that if deforestation due to ethanol production falls in the Midwest it causes larger land use emissions compared to the AEZ 7.

The bottom panel of Map 3 represents land use emissions factors for the pasture areas. In general, the land emissions factors of pasture areas are smaller than the forest areas in a same

region/AEZ. For example, the pasture land emissions factor of US AEZ 7 is about 101 Mg CO2 ha^{-1}. This is about one fourth of the forest emissions factor in this AEZ.

The model developed by Plevin et al. (2011) takes GTAP land use changes and calculates land use emissions in grams of CO_2 equivalent per megajoule (gCO_2eMJ^{-1}) of produced biofuel, ethanol in this case. The land use emissions calculated for the three simulation results are shown in table 6. This table indicates that increasing US ethanol production from its 2001 level to 15 billion gallons causes about 35.6 gCO_2eMJ^{-1} emissions, if there is no irrigation constraint across the world. Factoring in the physical limitations on irrigation expansion increases the land-based emissions to 45.4 gCO_2eMJ^{-1}. This means that the existing water scarcity adds 27.5% to the emissions due to land use changes induced by ethanol expansion. As shown in table 6 the *constrained* case also generates 27.5% more emissions compared to the *mingled* case where we only consider the mixed of irrigated and rainfed cropland. This means that earlier studies, which failed to distinguish rainfed from irrigated land, likely underestimated induced land use emissions due to ethanol production more than one-fifth.

Conclusions

In recent years numerous studies have examined the global land use changes and consequent emissions due to biofuel expansion across the world. These studies have effectively considered all cropland as being rainfed; thereby ignoring the role of irrigation in biofuel-induced land use changes. This paper develops a new general equilibrium framework which disaggregates irrigated and rainfed cropping industries to examine the role of potential irrigation constraints in biofuel induced land use changes. This study shows that models which ignore the role of irrigation and mingled irrigated and rainfed areas tend to systematically underestimate the induced land use changes due to US ethanol program by about 5.7%. The results also indicate

that expansion of irrigation could reduce the size of land requirement for ethanol production up to 18%. The model which ignores the role of irrigation in crop production also under-estimates induced land use emissions due to ethanol expansion by more than one-fifth.

References

Addams, L. and Boccaletti, G. and Kerlin, M. and Stuchtey, M. (2009). *Charting Our Water Future: Economic Frameworks to Inform Decision-making.* 2030 Water Resources Group and McKinsey and Company.

Alvaro, C., K. Rehdanz, and R, Tol. (2001). The GTAP-W Model: Accounting for Water Use in Agriculture. *GTAP Working Paper, Purdue University*.

Cai, X., and M. Rosegrant. (2002). Global Water Demand and Supply Projections Part 1.A Modeling Approach. *Water International, 27*(2), 159-169.

Dominguez-Faus, R., S. Powers, J. Burken, and J. Alverez. (2009). The Water Footprint of Biofuels: A Drink or Drive Issue? *Environmental Science and Technology, 43*(9), 3005-3010.

Fargione, J., J. Hill, D. Tilman, S. Polasky, and P. Hawthorne. (2008). Land Clearing and the Biofuel Carbon Debt. *Science, 319*(5867), 1235–1238.

Fraiture , C., M. Giordano, and Y. Liao. (2008). Biofuels and Implications for Agricultural Water Use: Blue Impacts of Green Energy. *Water Policy, 10*(1), 67–81.

Gurgel, A., J. Reilly, S. Paltsev. (2007). Potential Land Use Implications of a Global Biofuels Industry. *Journal of Agricultural and Food Industrial Organization, 5*(2), Article 9.

Hertel, T., A. Golub, A. Jones, M. O'Hare, R. Pelvin, and D. Kammen. (2010). Effects of US Maize Ethanol on Global Land Use and Greenhouse Gas Emissions: Estimating Market-Mediated Responses. *BioScience, 60*(3), 223-231.

Hoogeveen, J., J. Faures, and N. Giessen. (2009). Increased Biofuel Production in the Coming Decade: To What Extend Will It Affect Global Freshwater Resources? *Irrigation and Drainage, 58*(S1), S148–S160.

M., H. (2005). *SplitCom: Programs to Disaggregate a GTAP Sector.* Melbourne, Australia: Centre of Policy Studies, Monash University.

Monfreda, C., N. Ramankutty, and J. Foley. (2008). Farming the Planet: 2. Geographic Distribution of Crop Areas, Yields, Physiological Types, and Net Primary Production in the Year 2000. *Global Biogeochemical Cycles, 22*(GB1022).

Plevin, R., H. Gibbs, J. Duffy, S. Yui, S. Yeh. (2011). *Agro-ecological Zone Emission Factor Model.* California Air Resource Board.

Searchinger, T., R. Heimlich, R. Houghton , F. Dong, A. Elobeid, J. Fabiosa, S. Tokgoz , D. Hayes, T. Yu. (2008). Use of U.S. Croplands for Biofuels Increases Greenhouse Gases Through Emissions from Land-Use Change. *Science, 319*(5867), 1238-1240.

Siebert, S. and P. Döll. (2010). Quantifying Blue and Green Virtual Water Contents in Global Crop Production as well as Potential Production Losses without Irrigation. *Journal of Hydrology, 384*(3-4), 198-217.

Smarkhtin, V. (Oct. 13, 2011). *Water Management in Developing World: Adapting to Increases Variability and Changes.* Presentation at Stanford University.

Taheripour, F., T. Hertel, and W. Tyner. (2011). Implications of Biofuels Mandates for the Global Livestock Industry: a Computable General Equilibrium Analysis. *Agricultural Economics, 42*(3), 325-342.

Taheripour, F., T. Hertel, W. Tyner, J. Bechman, and D. Birur. (2010). Biofuels and Their By-Products: Global Economic and Environmental Implications. *Biomass and Bioenergy, 34*(3), 278-289.

Tyner, W., F. Taheripour, Q. Zhuang, D. Birur, and U. Baldos. (2010). *Land Use Changes and Consequent CO2 Emissions due to US Corn Ethanol Production: A Comprehensive Analysis.* Department of Agricultural Economics, Purdue University.

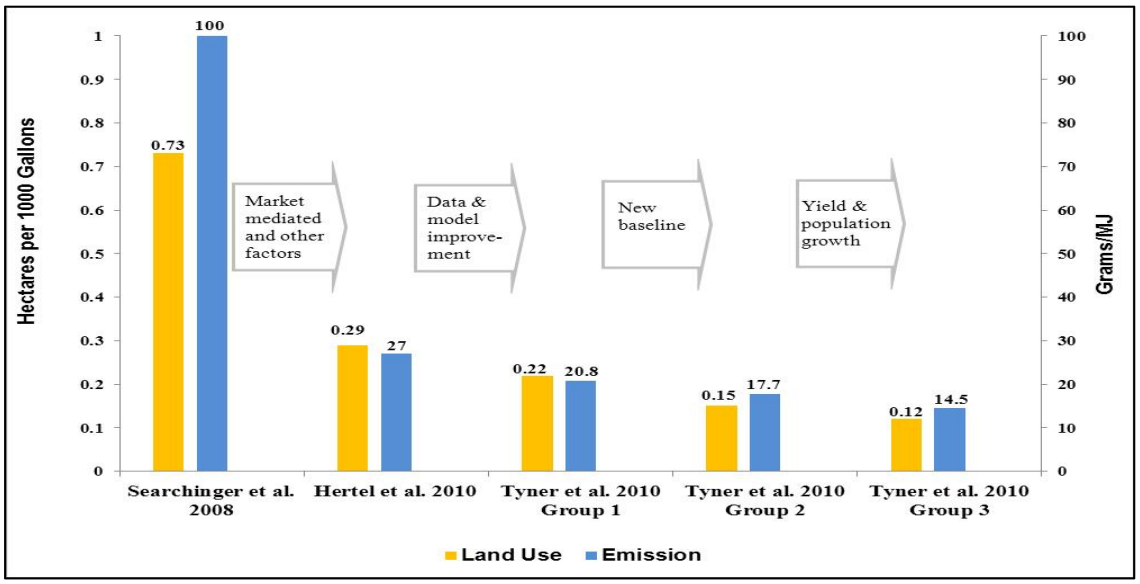

Figure 1. Estimates for additional land requirement and land use emissions due to US ethanol production

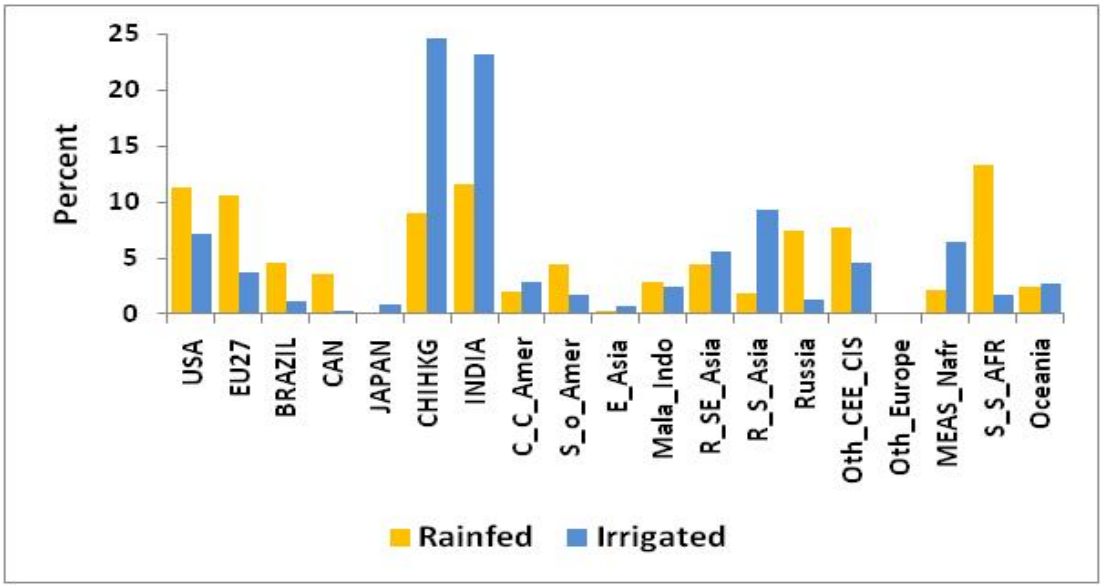

Figure 2. Global distribution of harvested area by irrigation type

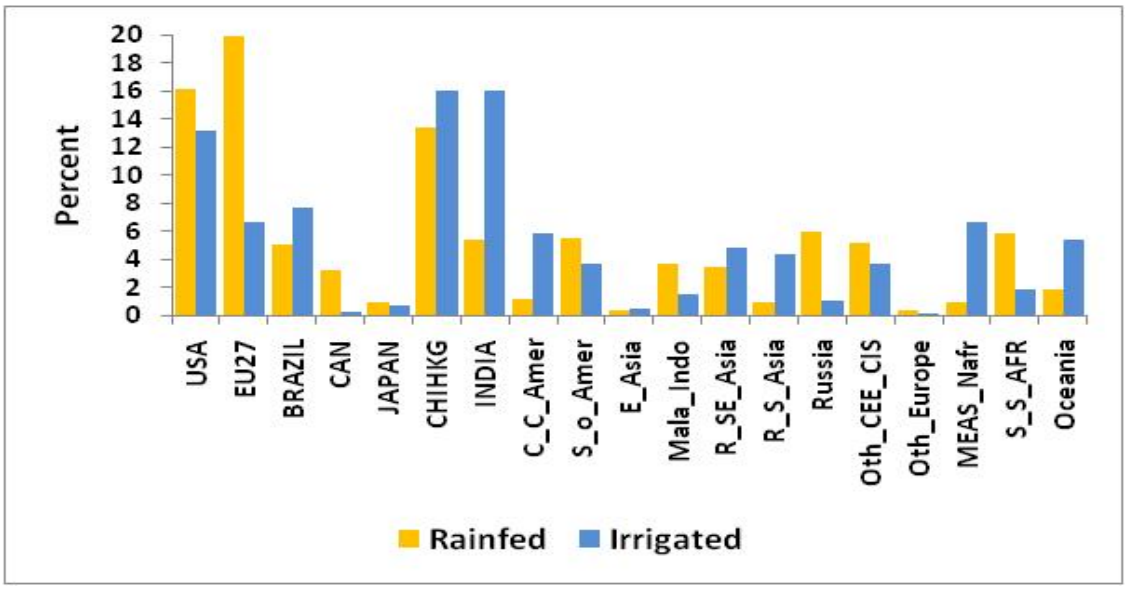

Figure 3. Global distribution of crop production by irrigation type

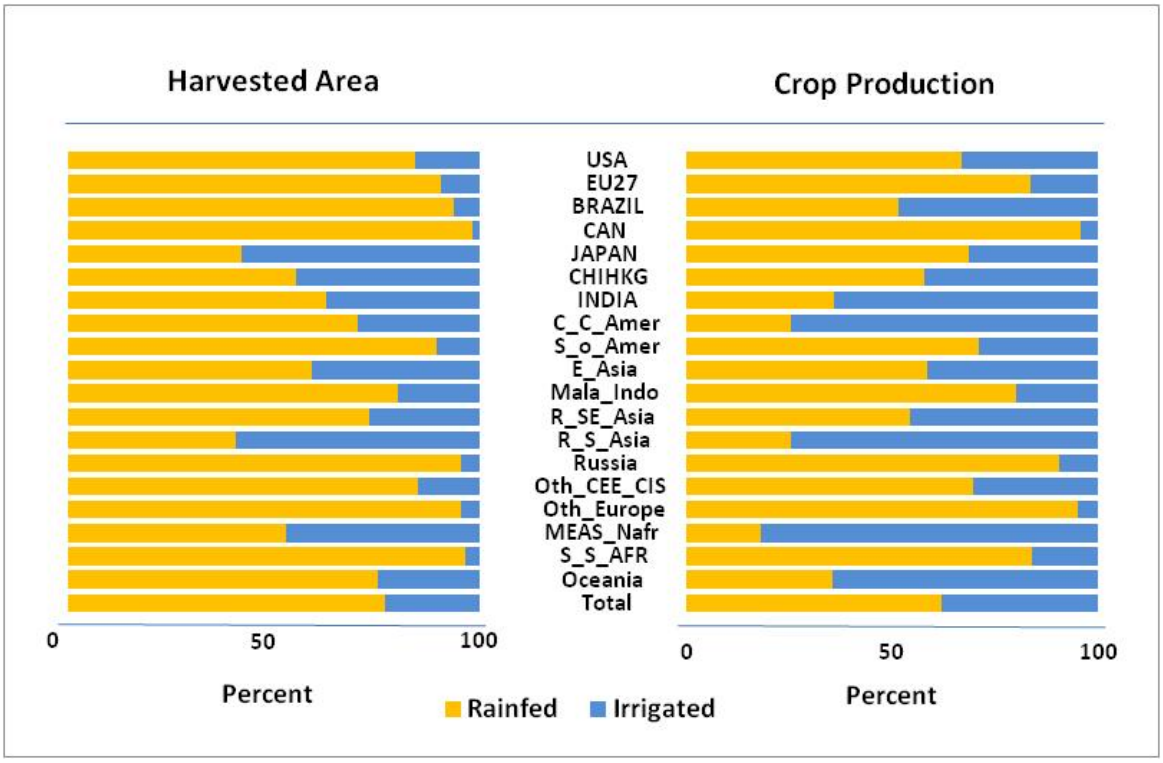

Figure 4. Harvested areas and crop production by region and by irrigation type

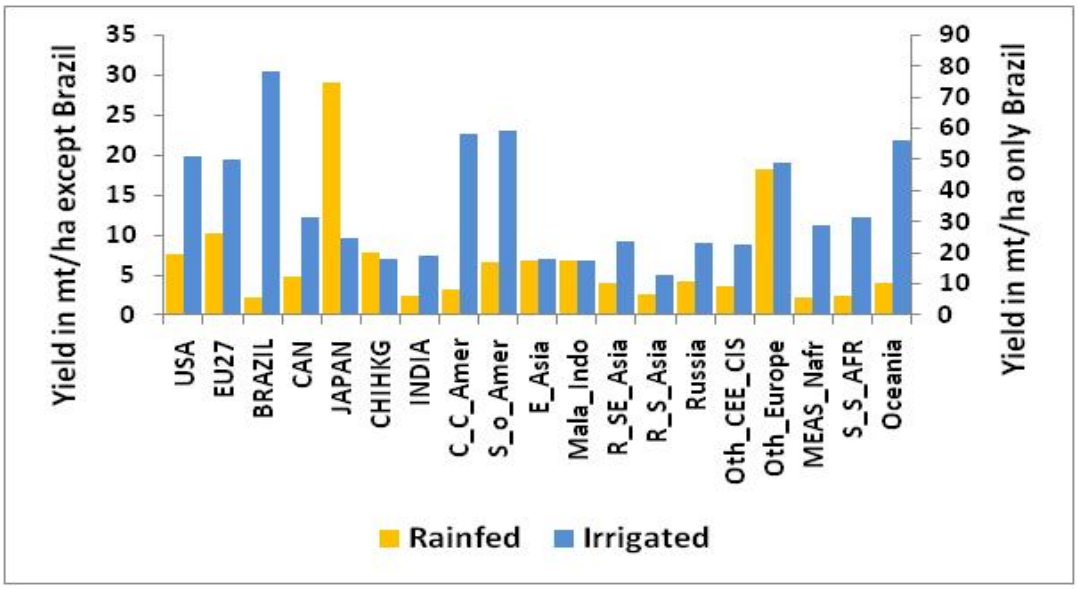

Figure 5. Irrigated and rainfed yields by region

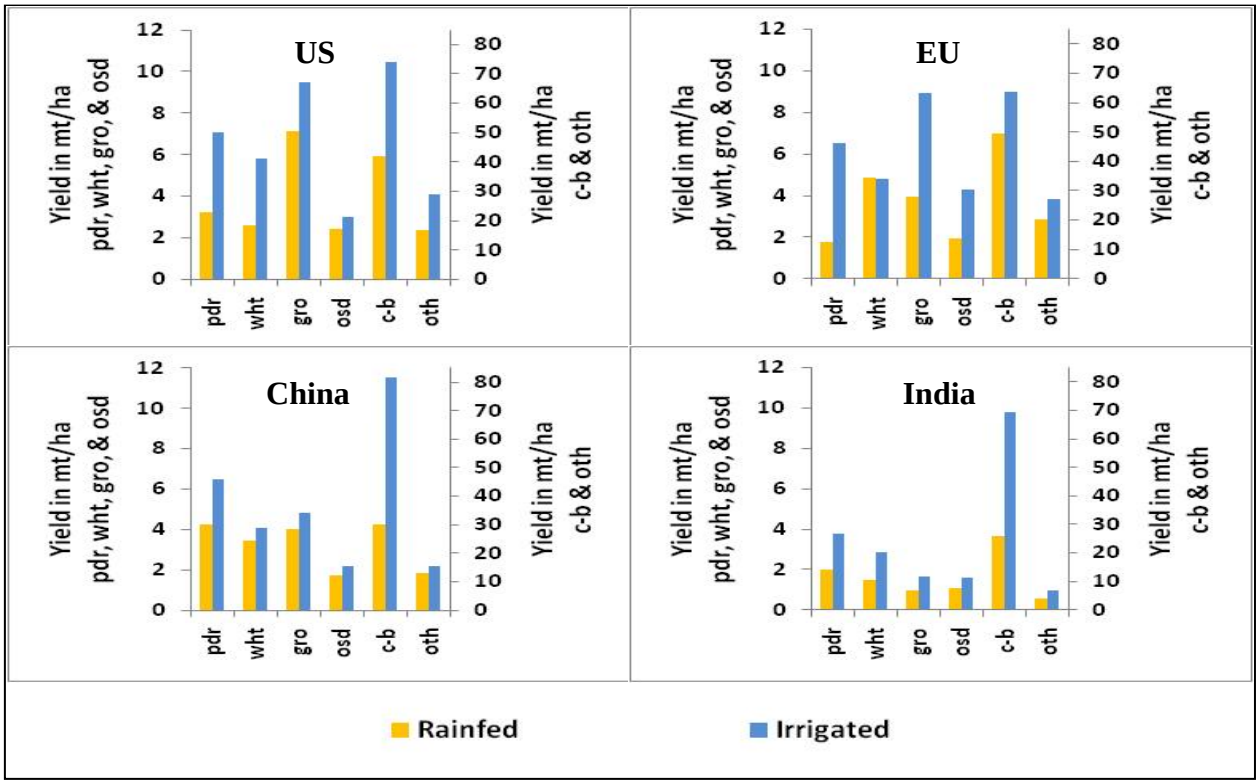

Figure 6. Irrigated and rainfed yields by crop types for selected regions

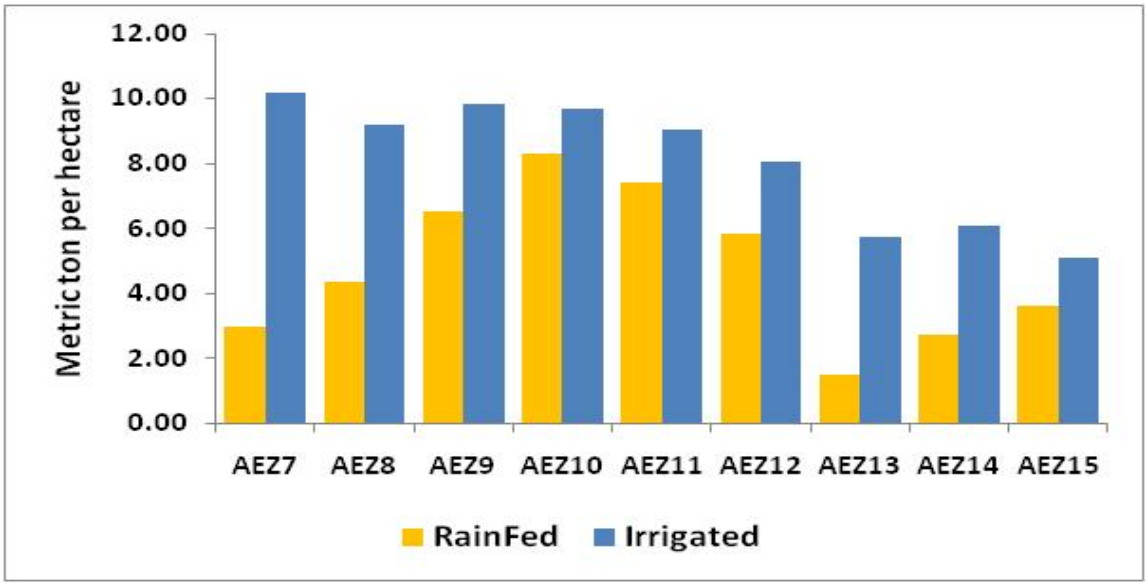

Figure 7. US coarse grains yields by irrigation type and AEZ

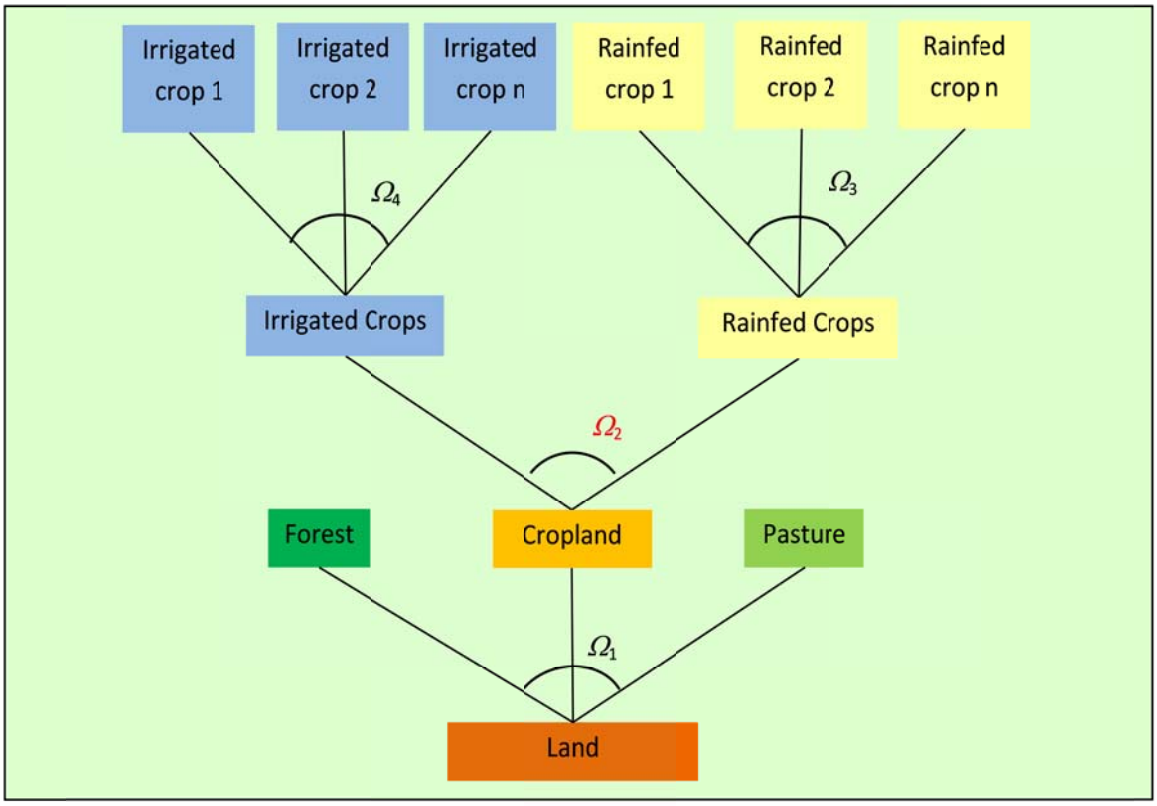

Figure 8. Modified land supply tree

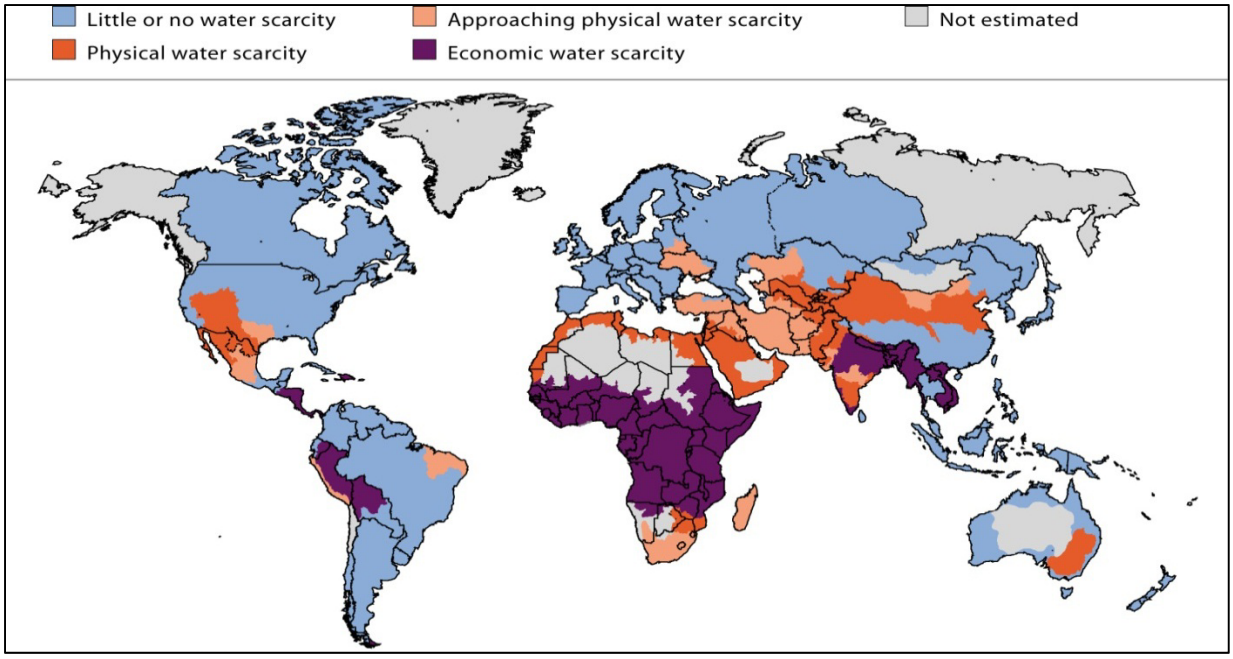

Map 1. Global water scarcity (Source: IWMI)

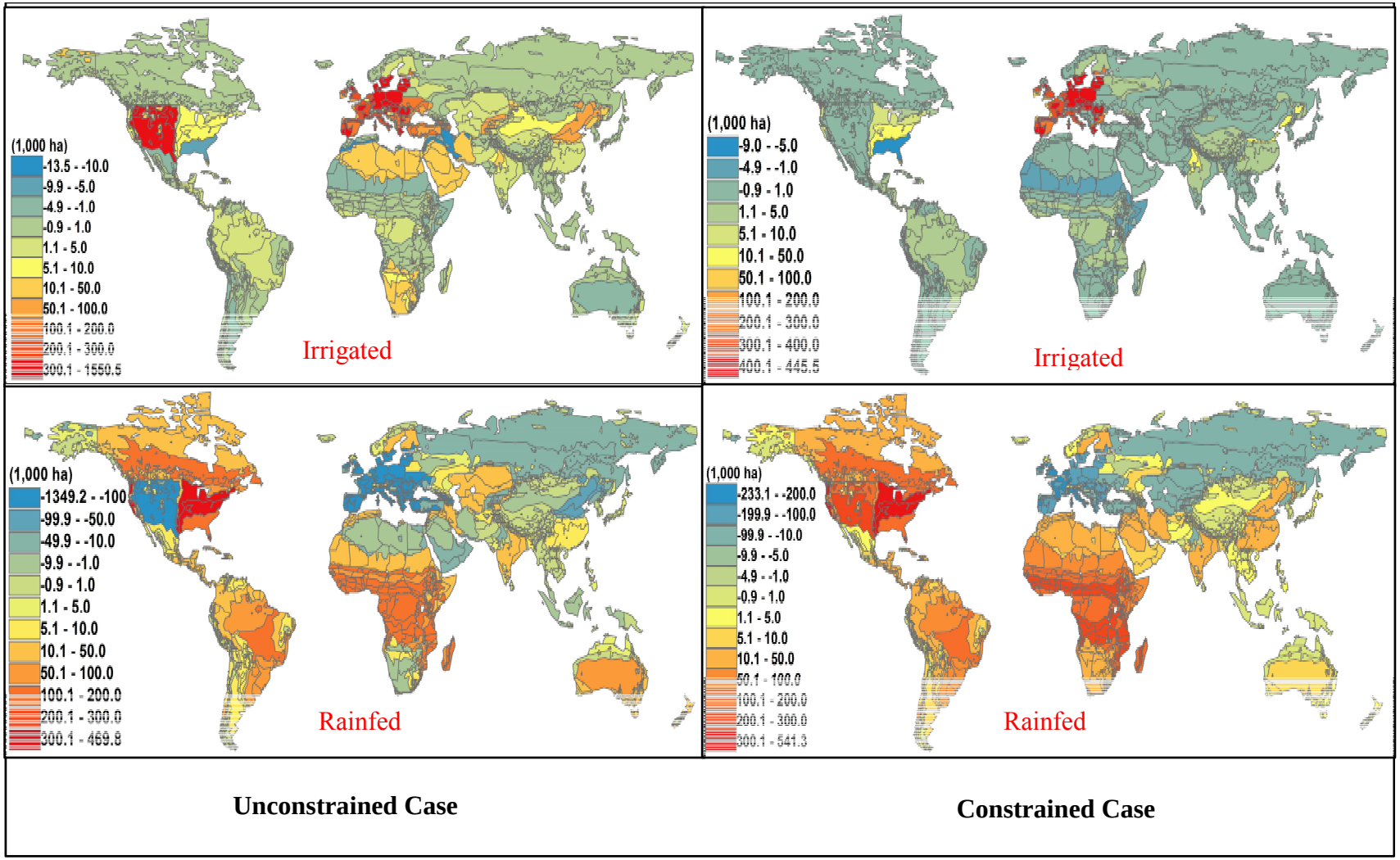

Map 2. Cropland cover changes with and without irrigation constraint*
* Figures represent change in harvested areas.

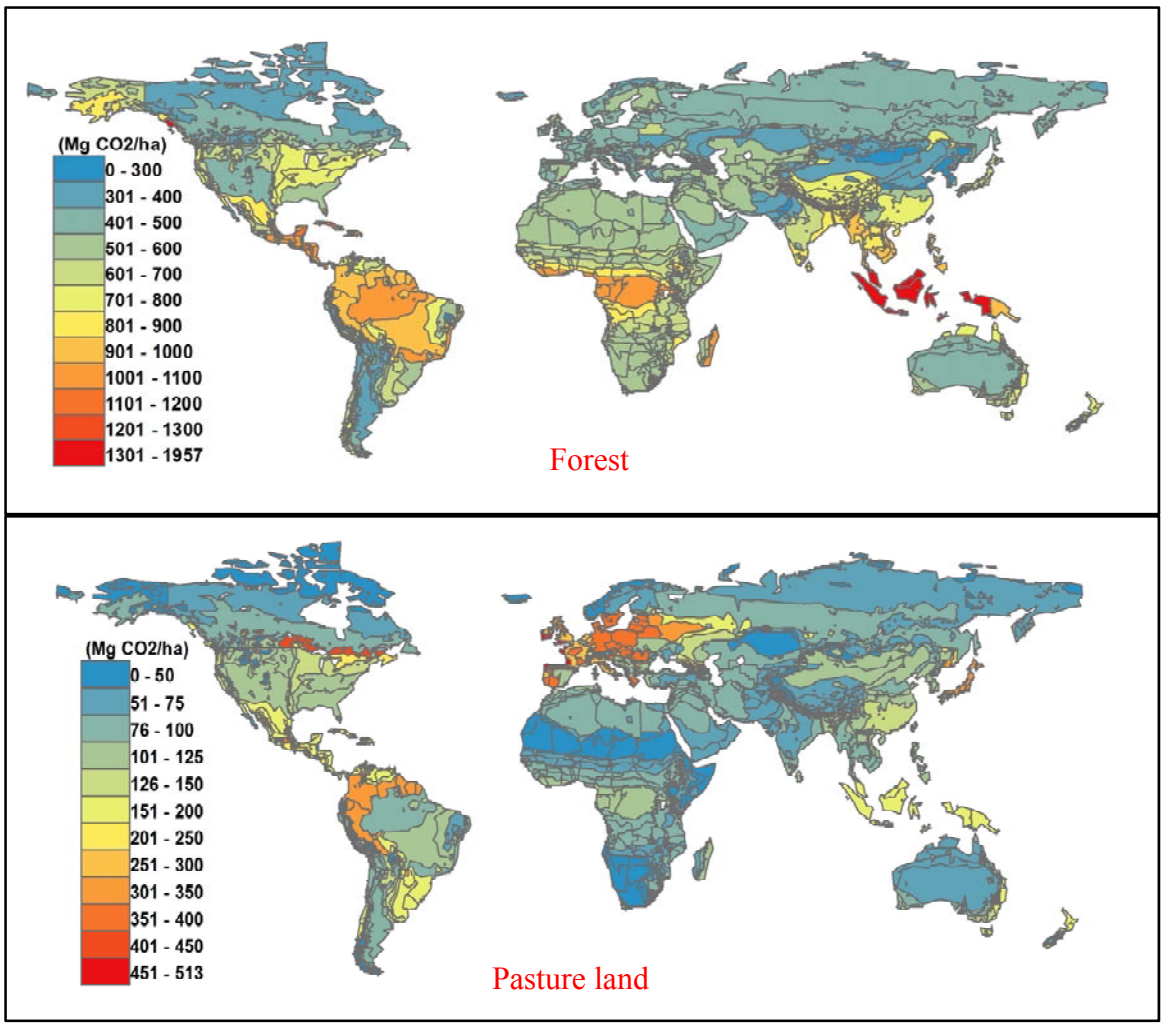

Map 3. Carbone fluxes (Mg CO_2 $ha^{-1}y^{-1}$) due to conversion of natural land to cropland (Source: Plevin et al. 2011)

Table 1. Irrigation constraint and land use changes due to US ethanol production (1000 hectares)

Regions	Unconstrained experiment		Mingled experiment		Constrained experiment	
	Hectare	Share%	Hectare	Share%	Hectare	Share%
USA	1333.0	35.5	1314.3	31.4	1671.2	37.7
EU27	353.6	9.4	423.2	10.1	450.3	10.2
BRAZIL	248.0	6.6	291.3	7.0	273.9	6.2
CAN	403.6	10.7	434.1	10.4	555.6	12.5
JAPAN	3.3	0.1	10.2	0.2	5.2	0.1
CHIHKG	35.4	0.9	53.7	1.3	100.0	2.3
INDIA	75.3	2.0	80.9	1.9	89.0	2.0
C_C_Amer	87.6	2.3	95.8	2.3	95.4	2.2
S_o_Amer	137.2	3.7	150.6	3.6	185.2	4.2
E_Asia	1.5	0.0	1.8	0.0	2.0	0.0
Mala_Indo	-4.6	-0.1	-2.0	0.0	0.4	0.0
R_SE_Asia	2.8	0.1	4.2	0.1	6.9	0.2
R_S_Asia	20.2	0.5	26.0	0.6	24.9	0.6
Russia	-11.7	-0.3	-13.4	-0.3	-29.5	-0.7
Oth_CEE_CIS	101.2	2.7	196.4	4.7	-272.3	-6.1
Oth_Europe	5.1	0.1	5.9	0.1	6.4	0.1
MEAS_NAfr	101.8	2.7	100.3	2.4	108.4	2.4
S_S_AFR	721.4	19.2	884.9	21.2	1126.5	25.4
Oceania	139.7	3.7	121.8	2.9	31.6	0.7
TOTAL	3754.5	100.0	4180.1	100.0	4430.8	100.0

Table 2. Irrigation constraint and shares of forest and pasture in land use changes due to US ethanol production (%)

Regions	Unconstrained experiment		Mingled experiment		Constrained experiment	
	Forest	Pasture	Forest	Pasture	Forest	Pasture
USA	51.0	49.0	39.5	60.5	51.1	48.9
EU27	64.4	35.6	65.0	35.0	64.3	35.7
Brazil	27.5	72.5	24.9	75.1	19.8	80.2
Other Regions	6.0	94.0	6.4	93.6	9.8	90.2
World	28.9	71.1	24.1	75.9	31.5	68.5

Table 3. Irrigated and rainfed cropland changes due to US ethanol production obtained from unconstrained and constrained experiments (1000 hectares)

Regions	Unconstrained		Constrained	
	Irrigated	Rainfed	Irrigated	Rainfed
USA	2166.5	-833.5	11.8	1659.3
EU27	828.6	-475.0	1094.8	-644.5
BRAZIL	3.5	244.5	3.9	270.0
CAN	6.3	397.2	6.4	549.3
JAPAN	0.8	2.5	1.3	3.9
CHIHKG	167.0	-131.5	62.5	37.5
INDIA	51.3	24.0	61.5	27.5
C_C_Amer	1.7	85.9	4.4	91.0
S_o_Amer	0.9	136.2	4.7	180.6
E_Asia	0.2	1.3	0.2	1.8
Mala_Indo	-0.2	-4.4	0.0	0.3
R_SE_Asia	0.2	2.6	0.6	6.3
R_S_Asia	3.6	16.6	1.3	23.6
Russia	4.9	-16.6	4.6	-34.1
Oth_CEE_CIS	354.8	-253.5	0.0	-272.3
Oth_Europe	0.1	5.1	0.1	6.3
MEAS_Nafr	57.6	44.2	0.0	108.4
S_S_AFR	54.9	666.4	4.1	1122.5
Oceania	-1.0	140.7	0.6	31.0
Total	3701.8	52.7	1262.6	3168.2

Table 4. Changes in US cropland by AEZ due to US ethanol production obtained from alternative experiments (1000 hectares)

AEZ	Unconstrained			Constrained		
	Irrigated	Rainfed	Total	Irrigated	Rainfed	Total
AEZ1	0.0	0.0	0.0	0.0	0.0	0.0
AEZ2	0.0	0.0	0.0	0.0	0.0	0.0
AEZ3	0.0	0.0	0.0	0.0	0.0	0.0
AEZ4	0.0	0.0	0.0	0.0	0.0	0.0
AEZ5	0.0	0.0	0.0	0.0	0.0	0.0
AEZ6	0.0	0.0	0.0	0.0	0.0	0.0
AEZ7	1550.5	-1349.2	201.3	0.0	291.7	291.7
AEZ8	580.6	-449.9	130.7	0.0	183.7	183.7
AEZ9	0.7	49.1	49.8	0.9	58.6	59.4
AEZ10	8.6	469.8	478.4	9.9	541.3	551.2
AEZ11	8.6	334.5	343.1	10.1	390.6	400.7
AEZ12	-6.5	125.7	119.2	-9.0	176.6	167.6
AEZ13	24.2	-18.4	5.8	0.0	11.6	11.6
AEZ14	-0.3	4.6	4.3	0.0	4.7	4.7
AEZ15	0.0	0.3	0.4	0.0	0.6	0.6
AEZ16	0.0	0.0	0.0	0.0	0.0	0.0
AEZ17	0.0	0.0	0.0	0.0	0.0	0.0
AEZ18	0.0	0.0	0.0	0.0	0.0	0.0
Total	2166.5	-833.5	1333.0	11.8	1659.3	1671.2

Table 5. Land use emissions due to US ethanol production

Simulations	Ethanol Production (billion gallons)	Annualized ILUC Emissions (gCO_2eMJ^{-1})	Deviation from Mingled
Unconstrained	13.23	35.6	0.0
Mingled	13.23	35.6	0.0
Constrained	13.23	45.4	27.5

Appendix A

Harvested area and crop production by irrigation type

In this appendix, we explain the process we followed to split the SAGE data set on harvested area and crop production documented in Monfreda et al. (2009) into irrigated and rainfed categories. To achieve this goal we used Siebert and Döll (2010) data on harvested area and yield by irrigation type. Henceforth we refer to their data set as S-D. This data set classifies global harvested area for 29 crop categories at 0.5^{o} x 0.5^{o} spatial resolution by irrigation type. It also provides information on crop yields by irrigation type for the 29 crop categories at the same spatial resolution.

We began with the S-D data at the grid cell level. Given the harvested area and yield by irrigation type we used the following relationship to calculate gridded crop production by irrigation type for the 29 crop categories:

$$Q_{ij}^{w} = A_{ij}^{w} \cdot Y_{ij}^{w}$$

Here Q, A, and Y represent crop quantity, harvested area, and yield. The superscript w denotes irrigation type with: with either w = irrigated or w = rainfed, i indicates crop type with 29 members based on S-D, and j shows the index of grid cell for all grid cells available in S-D data set.

We then matched S-D grid cells with the GTAP-AEZ profile at the grid cell to aggregate harvested areas and quantities of crops up to country by AEZ level. The mapping schedule presented in Table A1 was then used to match the S-D 29 crop categories with SAGE crop categories aggregated to 8 crop categories which we use in GTAP Data Base. Using this mapping schedule we aggregated the S-D data set to the 8 SAGE /GTAP crop categories. Then we used the following relationships to split harvested area and crop production of SAGE/GTAP data into irrigated and rainfed categories:

$$Q_{irz}^{w^{SAGE}} = \left[\frac{Q_{irz}^{w^{S-D}}}{\sum_w Q_{irz}^{w^{S-D}}}\right] \cdot Q_{irz}^{SAGE}$$

$$A_{irz}^{w^{SAGE}} = \left[\frac{A_{irz}^{w^{S-D}}}{\sum_w A_{irz}^{w^{S-D}}}\right] \cdot A_{irz}^{SAGE}$$

These two equations serve to 'share out' quantity produced and area harvested in the SAGE data base into irrigated and rainfed components. Specifically, *Q* and *A* represent crop quantity and harvested area, *w* shows the index of irrigation type with two categories of irrigated and rainfed, *i* indicates crop type with 8 members, and *r* shows the index of region for all region in the data set, *z* is the index of AEZ from 1 to 18, and finally *S-D* and *SAGE* represent their corresponding data sets.

Finally, the results obtained from the above step are aggregated to the 19 model regions which we use in this paper. Tables A2 and A3 report the results of this splitting process for harvested areas and crop production by irrigation type by the 19 regions which we use in this paper.

Table A1. S-D and SAGE crop categories

S-D crop categories	GTAP/SAGE crop categories	S-D crop categories	GTAP/SAGE crop categories
Wheat	wht	Groundnuts / Peanuts	osd
Maize for grain	gro	Pulses	v-f
Rice	pdr	Citrus	v-f
Barley	gro	Date palm	v-f
Rye for grain	gro	Grapes / vine	v-f
Millet	gro	Cotton	pfb
Sorghum for grain	gro	Cocoa	ocr
Soybeans	osd	Coffee	ocr
Sunflower	osd	Others perennial	ocr
Potatoes	v-f	Managed grassland/pasture	ocr
Cassava	v-f	Others annual	ocr
Sugar cane	c-b	Maize, forage	ocr
Sugar beets	c-b	Rye, forage	ocr
Oil palm	osd	Sorghum, forage	ocr
Rapeseed / canola	osd		

Table A2. Geographical distribution of land by irrigation type

Region	Area (million hectares)			Distribution by irrigation (%)			Geographical distribution (%)		
	Rainfed	Irrigated	Total	Rainfed	Irrigated	Total	Rainfed	Irrigated	Total
USA	111.1	21.0	132.0	84.1	15.9	100.0	11.3	7.2	10.3
EU27	104.2	10.8	115.0	90.6	9.4	100.0	10.6	3.7	9.0
BRAZIL	45.4	3.1	48.5	93.5	6.5	100.0	4.6	1.1	3.8
CAN	34.7	0.6	35.3	98.3	1.7	100.0	3.5	0.2	2.8
JAPAN	1.8	2.4	4.2	42.0	58.0	100.0	0.2	0.8	0.3
CHIHKG	88.8	72.1	160.9	55.2	44.8	100.0	9.0	24.6	12.6
INDIA	114.2	68.0	182.2	62.7	37.3	100.0	11.6	23.2	14.3
C_C_Amer	19.4	8.2	27.6	70.1	29.9	100.0	2.0	2.8	2.2
S_o_Amer	43.5	5.1	48.6	89.4	10.6	100.0	4.4	1.8	3.8
E_Asia	3.0	2.1	5.0	59.1	40.9	100.0	0.3	0.7	0.4
Mala_Indo	28.5	7.1	35.6	80.0	20.0	100.0	2.9	2.4	2.8
R_SE_Asia	44.2	16.4	60.6	73.0	27.0	100.0	4.5	5.6	4.7
R_S_Asia	18.7	27.1	45.8	40.8	59.2	100.0	1.9	9.2	3.6
Russia	72.9	3.6	76.5	95.3	4.7	100.0	7.4	1.2	6.0
Oth_CEE_CIS	75.3	13.6	88.9	84.8	15.2	100.0	7.7	4.6	7.0
Oth_Europe	1.0	0.1	1.1	95.3	4.7	100.0	0.1	0.0	0.1
MEAS_Nafr	21.1	18.9	40.0	52.7	47.3	100.0	2.1	6.5	3.1
S_S_AFR	131.0	4.9	135.9	96.4	3.6	100.0	13.3	1.7	10.7
Oceania	24.2	8.0	32.1	75.2	24.8	100.0	2.5	2.7	2.5
Total	982.8	293.1	1275.9	77.0	23.0	100.0	100.0	100.0	100.0

Table A3. Geographical distribution of crop production by irrigation type

Region	Production (million metric tons)			Distribution by irrigation (%)			Geographical distribution (%)		
	Rainfed	Irrigated	Total	Rainfed	Irrigated	Total	Rainfed	Irrigated	Total
USA	839.7	417.2	1256.8	66.8	33.2	100.0	16.2	13.1	15.0
EU27	1064.5	210.9	1275.3	83.5	16.5	100.0	20.5	6.6	15.2
BRAZIL	261.1	245.0	506.1	51.6	48.4	100.0	5.0	7.7	6.0
CAN	165.0	7.5	172.5	95.7	4.3	100.0	3.2	0.2	2.1
JAPAN	50.9	23.4	74.3	68.5	31.5	100.0	1.0	0.7	0.9
CHIHKG	696.4	507.8	1204.1	57.8	42.2	100.0	13.4	16.0	14.4
INDIA	283.4	509.3	792.7	35.7	64.3	100.0	5.5	16.0	9.5
C_C_Amer	63.2	186.6	249.7	25.3	74.7	100.0	1.2	5.9	3.0
S_o_Amer	286.6	118.0	404.6	70.8	29.2	100.0	5.5	3.7	4.8
E_Asia	20.5	14.5	34.9	58.6	41.4	100.0	0.4	0.5	0.4
Mala_Indo	191.1	48.0	239.1	79.9	20.1	100.0	3.7	1.5	2.9
R_SE_Asia	179.4	151.6	331.0	54.2	45.8	100.0	3.5	4.8	4.0
R_S_Asia	46.8	137.6	184.5	25.4	74.6	100.0	0.9	4.3	2.2
Russia	310.2	32.8	343.0	90.4	9.6	100.0	6.0	1.0	4.1
Oth_CEE_CIS	268.5	118.1	386.6	69.5	30.5	100.0	5.2	3.7	4.6
Oth_Europe	18.7	1.0	19.7	95.0	5.0	100.0	0.4	0.0	0.2
MEAS_Nafr	47.2	212.7	259.8	18.1	81.9	100.0	0.9	6.7	3.1
S_S_AFR	305.4	59.5	365.0	83.7	16.3	100.0	5.9	1.9	4.4
Oceania	94.6	173.3	267.9	35.3	64.7	100.0	1.8	5.5	3.2
Total	5193.0	3174.6	8367.6	62.1	37.9	100.0	100.0	100.0	100.0

Appendix B

Regions and their members

Table B 1. Regions and their members

Region	Description	Corresponding Countries in GTAP
USA	United States	usa
EU27	European Union 27	aut, bel, bgr, cyp, cze, deu, dnk, esp, est, fin, fra, gbr, grc, hun, irl, ita, ltu, lux, lva, mlt, nld, pol, prt, rom, svk, svn, swe
BRAZIL	Brazil	bra
CAN	Canada	can
JAPAN	Japan	jpn
CHIHKG	China and Hong Kong	chn, hkg
INDIA	India	ind
C_C_Amer	Central and Caribbean Americas	mex, xna, xca, xfa, xcb
S_o_Amer	South and Other Americas	col, per, ven, xap, arg, chl, ury, xsm
E_Asia	East Asia	kor, twn, xea
Mala_Indo	Malaysia and Indonesia	ind, mys
R_SE_Asia	Rest of South East Asia	phl, sgp, tha, vnm, xse
R_S_Asia	Rest of South Asia	bgd, lka, xsa
Russia	Russia	rus
Oth_CEE_CIS	Other East Europe and Rest of Former Soviet Union	xer, alb, hrv, xsu, tur
R_Europe	Rest of European Countries	che, xef
MEAS_NAfr	Middle Eastern and North Africa	xme,mar, tun, xnf
S_S_AFR	Sub Saharan Africa	bwa, zaf, xsc, mwi, moz, tza, zmb, zwe, xsd, mdg, uga, xss
Oceania	Oceania countries	aus, nzl, xoc